Brain Structure and Function (2020) 225:1073–1088
https://doi.org/10.1007/s00429-020-02059-w

ORIGINAL ARTICLE

In vivo reduction of striatal D1R by RNA interference alters expression of D1R signaling-related proteins and enhances methamphetamine addiction in male rats

Alison D. Kreisler[1] · Michael J. Terranova[1] · Sucharita S. Somkuwar[1] · Dvijen C. Purohit[1] · Shanshan Wang[1,2] · Brian P. Head[1,2] · Chitra D. Mandyam[1,2]

Received: 9 October 2019 / Accepted: 18 March 2020 / Published online: 3 April 2020

Abstract

This study sought to determine if reducing dopamine D1 receptor (D1R) expression in the dorsal striatum (DS) via RNA-interference alters methamphetamine self-administration. A lentiviral construct containing a short hairpin RNA (shRNA) was used to knock down D1R expression (D1RshRNA). D1RshRNA in male rats increased responding for methamphetamine (i.v.) under a fixed-ratio schedule in an extended access paradigm, compared to D1R-intact rats. D1RshRNA also produced a vertical shift in a dose–response paradigm and enhanced responding for methamphetamine in a progressive-ratio schedule, generating a drug-vulnerable phenotype. D1RshRNA did not alter responding for sucrose (oral) under a fixed-ratio schedule compared to D1R-intact rats. Western blotting confirmed reduced D1R expression in methamphetamine and sucrose D1RshRNA rats. D1RshRNA reduced the expression of PSD-95 and MAPK-1 and increased the expression of dopamine transporter (DAT) in the DS from methamphetamine, but not sucrose rats. Sucrose density gradient fractionation was performed in behavior-naïve controls, D1RshRNA- and D1R-intact rats to determine the subcellular localization of D1Rs, DAT and D1R signaling proteins. D1Rs, DAT, MAPK-1 and PSD-95 predominantly localized to heavy fractions, and the membrane/lipid raft protein caveolin-1 (Cav-1) and flotillin-1 were distributed equally between buoyant and heavy fractions in controls. Methamphetamine increased localization of PSD-95, Cav-1, and flotillin-1 in D1RshRNA and D1R-intact rats to buoyant fractions. Our studies indicate that reduced D1R expression in the DS increases vulnerability to methamphetamine addiction-like behavior, and this is accompanied by striatal alterations in the expression of DAT and D1R signaling proteins and is independent of the subcellular localization of these proteins.

Keywords Dopamine D1 receptors · Sucrose density gradient · MAPK-1 · Caveolin-1 · PSD-95 · Dopamine transporter

Introduction

Mesencephalic dopamine signaling plays important roles in the coordination of motivated and emotional behaviors, including drug taking. Commonly abused psychostimulants, including methamphetamine, act as indirect D1R agonists, and D1R-knockout mice fail to self-administer cocaine compared to wild-type controls (Caine et al. 2007). Furthermore, systemic blockade of D1R decreased methamphetamine-associated behavioral sensitization, conditioned place preference, reduced methamphetamine self-administration and reduced methamphetamine priming-induced drug-seeking (Bardo et al. 1999; Mizoguchi et al. 2004; Brennan et al. 2009; Carati and Schenk 2011; Nguyen et al. 2016). These studies suggest that D1R plays an important role in the rewarding properties of methamphetamine. However, the relevant brain population of D1R as well as the molecular mechanisms underlying such properties are unknown.

In the dorsal striatum (DS), D1Rs reside on a subset of medium spiny neurons (MSNs) that project to substantia nigra [known as the direct pathway (Gerfen and Young 1988; Ince et al. 1997)]. Exposure to psychostimulants increases the expression of striatal D1Rs (Worsley et al. 2000; Segal et al. 2005; Somkuwar et al. 2016). Loss of function studies

✉ Chitra D. Mandyam
cmandyam@scripps.edu

[1] VA San Diego Healthcare System, San Diego, CA 92161, USA

[2] Department of Anesthesiology, University of California San Diego, San Diego, CA 92161, USA

have shown that D1R-expressing MSNs are necessary for the complete expression of psychostimulant seeking, behavioral sensitization, and conditioned place preference (Lobo et al. 2010; Lobo and Nestler 2011). A causal role for D1Rs in the DS in psychostimulant addictive-like behavior has yet to be elucidated.

Our recent study has shown that progressive increases in the intake of methamphetamine over extended access schedules of reinforcement lead to escalated and unregulated intake of methamphetamine, increased D1R expression, and altered MAPK-1 activation in DS (Somkuwar et al. 2016). Systemic D1R antagonism in methamphetamine-experienced animals prevents methamphetamine-induced hyperphosphorylation of MAPK-1 in the DS and methamphetamine reward (Mizoguchi et al. 2004). Together these studies suggest that altered MAPK-1 activity by methamphetamine via aberrant D1R expression is an intracellular signal transduction mechanism contributing to the maladaptive plasticity associated with reinforcing effects of methamphetamine (Nestler 2001; Ahmed and Koob 2004; Brennan et al. 2009).

The association of D1Rs with membrane/lipid rafts (Kong et al. 2007; Voulalas et al. 2011; Yu et al. 2013)—specialized subcellular structures enriched in cholesterol and sphingolipid, and the cholesterol binding and scaffolding proteins caveolin-1 (Cav-1) and flotillin-1 (Evans et al. 2003; Rajendran et al. 2007; Stary et al. 2012)—has supported the speculation that dopamine receptor (DR) subtypes may be differentially distributed within and outside lipid rafts, such that their subcellular localization may have relevance to the signaling and modulation of synaptic dopamine (Dumartin et al. 2000; Sun et al. 2003; He et al. 2009). Furthermore, functioning and sensitivity of D1Rs are modulated by dopamine transporters [DAT; (Gross et al. 2011; Bai et al. 2014; Sase et al. 2016; Robison et al. 2017)], and mechanistic studies support the role of DAT in the modulation of synaptic dopamine and signaling of dopamine via D1Rs (Jones et al. 1998; Salahpour et al. 2008; Ghisi et al. 2009). Most notable is that DAT is trafficked to lipid rafts and subcellular localization of DAT may have relevance to the signaling and modulation of synaptic dopamine (Cremona et al. 2011). Additional mechanistic studies have indicated that lipid raft protein Cav-1 is directly regulated by MAPK-1, where hyperphosphorylation of MAPK-1 downregulates expression and function of Cav-1 (Engelman et al. 1999; Cohen et al. 2003). Psychostimulants and opiates regulate the expression of Cav-1 (Chakrabarti et al. 2016; Somkuwar et al. 2016; Cui et al. 2018), suggesting that interactions of D1Rs with Cav-1 may contribute to the behavioral effects of these drugs.

Together, these studies lead us to the mechanistic hypothesis that D1Rs in the DS are required for the escalation of methamphetamine self-administration, such that site-specific knockdown of D1Rs in the DS would reduce escalation of methamphetamine self-administration. Based on the hypothesis that D1Rs in methamphetamine-experienced rats are functionally impaired, and D1R dysfunction is associated with altered activity of MAPK-1 (Haberny et al. 2004; Mizoguchi et al. 2004; Jiao et al. 2007; Chen et al. 2009), altered expression of PSD-95 (Yao et al. 2004; Porras et al. 2012; Fasano et al. 2013; Zhang et al. 2014), DAT (Ghisi et al. 2009; Sun et al. 2012; Rui et al. 2013) and Cav-1 (Kong et al. 2007; Voulalas et al. 2011) our studies quantified the striatal expression of these signaling proteins. Lastly, since D1Rs, Cav-1, flotillin-1, and DAT are trafficked to lipid rafts and their subcellular localization may regulate the signaling and modulation of synaptic dopamine, and behavioral responses to methamphetamine, we evaluated the expression of these signaling molecules in lipid raft (buoyant) and non-lipid raft (heavy) sucrose density gradient fractions.

Materials and methods

Animals

Experimental procedures were carried out in strict adherence to the NIH Guide for the Care and Use of Laboratory Animals and approved by the Institutional Animal Care and Use Committee of VA San Diego Healthcare System. Fifty-six adult male rats on a Long–Evans background (bred at the VA Vivarium), age matched, weighing 200–250 g and 7 weeks old at the start of the experiment, were housed two per cage in a temperature-controlled vivarium under a reverse light/dark cycle (lights off 8:00 AM–8:00 PM).

Viral vector construction, surgery, and viral gene transfer

Lentivirus (LV)-shD1R (D1RshRNA) was generated at the UCSD viral vector core facility using methods based on (Mastrangelo et al. 2012). The sequence for shRNA targeting D1R was chosen based on a recent publication that validated D1R silencing in adult rat brain (Noori-Daloii et al. 2012), and was modified to produce greater selectivity to rat D1R gene based on BLOCKiT™ RNAi Designer tool from Invitrogen (sequence used: 5′ GGTCCAAGGTGACCAACT TC T 3′). This sequence produced almost 30% reduction in D1R protein expression in LV-shD1R compared with LV-sh scrambled (shSRM, D1R-intact) controls when validated via Western blotting, 6 weeks post-LV injections. LV vectors were produced by transient co-transfection of HEK293T cells maintained in DMEM with 10% FCS as described previously (Head et al. 2011). Viral titer of ~ 10^{11} viral particle/μL was used. For stereotactic injections, forty-seven rats (7 weeks old) were anesthetized with 2–4% isoflurane mixed with oxygen. Using standard stereotaxic procedures (Galinato et al. 2018a), 30-gauge stainless steel injectors

were placed above the targeted brain region. Stereotaxic bilateral infusions of LV-shD1R and LV-shSRM with a GFP reporter sequence or sham (virus naïve) were applied to the DS (AP, 0.2 mm from bregma; ML, ± 2.3 mm from bregma; DV, − 4.5, − 5.1, and − 5.4 from dura) with a stainless steel injector attached to a syringe pump connected by plastic tubing (Fig. 1a–c). Infusions occurred at a flow rate of 1 µl/min with a total volume of 10 µl (3.5ul infused at − 4.5 mm, 4.5 µl infused at − 5.1 mm, and 2 µl infused at − 5.4 mm) per side. The injector was left in place an additional 5 min to minimize diffusion up the injector tract. Immediately after surgery, Flunixin® (2.5 mg/kg, s.c.) was given as analgesic, and Cefazolin was administered as antibiotic. For all experiments, accuracy of injection coordinates was confirmed by visualization of GFP-expressing cells in 40 um tissue sections (Fig. 1d–e). Four weeks following LV injections, rats either underwent surgery for jugular vein catheter implantation (for methamphetamine self-administration) or did not undergo any additional surgery (intended for sucrose self-administration/drinking; Fig. 1a).

Intravenous methamphetamine self-administration

Intravenous catheterization surgery: Twenty-five rats [fifteen D1RshRNA, ten D1R-intact (two LV-shSRM and eight sham/virus naïve)] underwent surgery for catheter implantation for intravenous self-administration 4–5 weeks after virus injections. Surgery, catheter maintenance and catheter patency were performed according to our previous publications (Mandyam et al. 2007; Galinato et al. 2015).

Training and maintenance on the extended access schedule (days 1–10)**:** one week after i.v. surgeries, all rats were trained to press a lever according to fixed-ratio 1 (FR1) schedule of methamphetamine reinforcement (0.05 mg/kg/injection of methamphetamine (provided by NIDA)) in operant boxes (Med Associates) under extended access conditions (6 h access per day for 10 days), hereafter referred to as the maintenance phase (Fig. 1a). A response on the active lever resulted in a 4-s infusion (90–100 µL of methamphetamine), followed by a 20-s timeout period to prevent overdose. Each infusion was paired for 4 s with white stimulus light over the active lever. Responses during the timeout or on the inactive lever were recorded but resulted in no programmed consequences. All animals increased methamphetamine self-administration across the maintenance phase (Fig. 2a). FR data were analyzed as number of reinforced (Fig. 2a, c) or non-reinforced (i.e., during the timeout period, Fig. 2b) active lever presses per session.

Dose–response (days 11–14): following ten sessions, animals underwent dose–response studies in which the methamphetamine dose administered was changed each day: 0.01, 0.05, 0.1, and 0.2 mg/kg/injection (within subjects). Dose–response sessions were maintained at 6 h and FR1 schedule.

Progressive ratio (day 15): the following day after dose–response sessions, responding was reinforced on a progressive ratio (PR) schedule of reinforcement (Richardson and Roberts 1996). On this schedule, the number of responses required for reinforcement increased progressively, and each session continued until a breakpoint (defined as the number of infusions obtained before 1 h elapsed with no infusions) was reached. For example, in the PR schedule, the response requirement began at 1 response/injection and increased according to the following equation: responses/injection = (5 × e(injection number × 0.2)) − 5. When a rat failed to achieve the response requirement within 1 h, the session ended. Sessions were capped at 6 h; however, no PR session exceeded 3 h. Breakpoints were determined for 0.05 mg/kg/injection. PR data were analyzed as the average cumulative active lever responses across sessions (Fig. 2d).

Sucrose self-administration

Training and maintenance on the limited access schedule (days 1–10)**:** a separate group of 22 rats also underwent stereotaxic surgery as described above [ten D1RshRNA, twelve D1R-intact (eight LV-shSRM and four sham/virus naïve)]. These rats were then trained to orally self-administer sucrose solution (10% w/v, 30 min sessions, under FR1 schedule) for ten sessions. Before sucrose sessions began, animals received two training sessions that were conducted overnight in the operant chambers, and active lever presses were rewarded with tap water (100 µl per reinforced response). This allowed us to determine whether the animal learned to (1) press the correct lever for a fluid reward and (2) drink the administered fluid from the delivery/sipper cup. All animals distinguished the active versus the inactive lever and consumed tap water dispensed during the water training sessions (data not shown). During 30-min sucrose sessions, 100 µl of 10% sucrose was delivered following an active lever press (similar to methamphetamine sessions, a response on the active lever resulted in a delivery into a sipper cup, followed by a 20-s time-out period). Each delivery was paired for 1 s with white stimulus light over the active lever. Response during the time-out or on the inactive lever was recorded but resulted in no programmed consequences). Operant sessions were conducted for a total of ten sessions.

Progressive ratio (day 11): the following day after the last FR session, responding was reinforced on a PR schedule of reinforcement (Richardson and Roberts 1996). On this schedule, the number of responses required for reinforcement increased progressively, and each session continued until a breakpoint (defined as the number of infusions obtained before 1 h elapsed with no infusions) was reached. Breakpoints were determined for 10% sucrose.

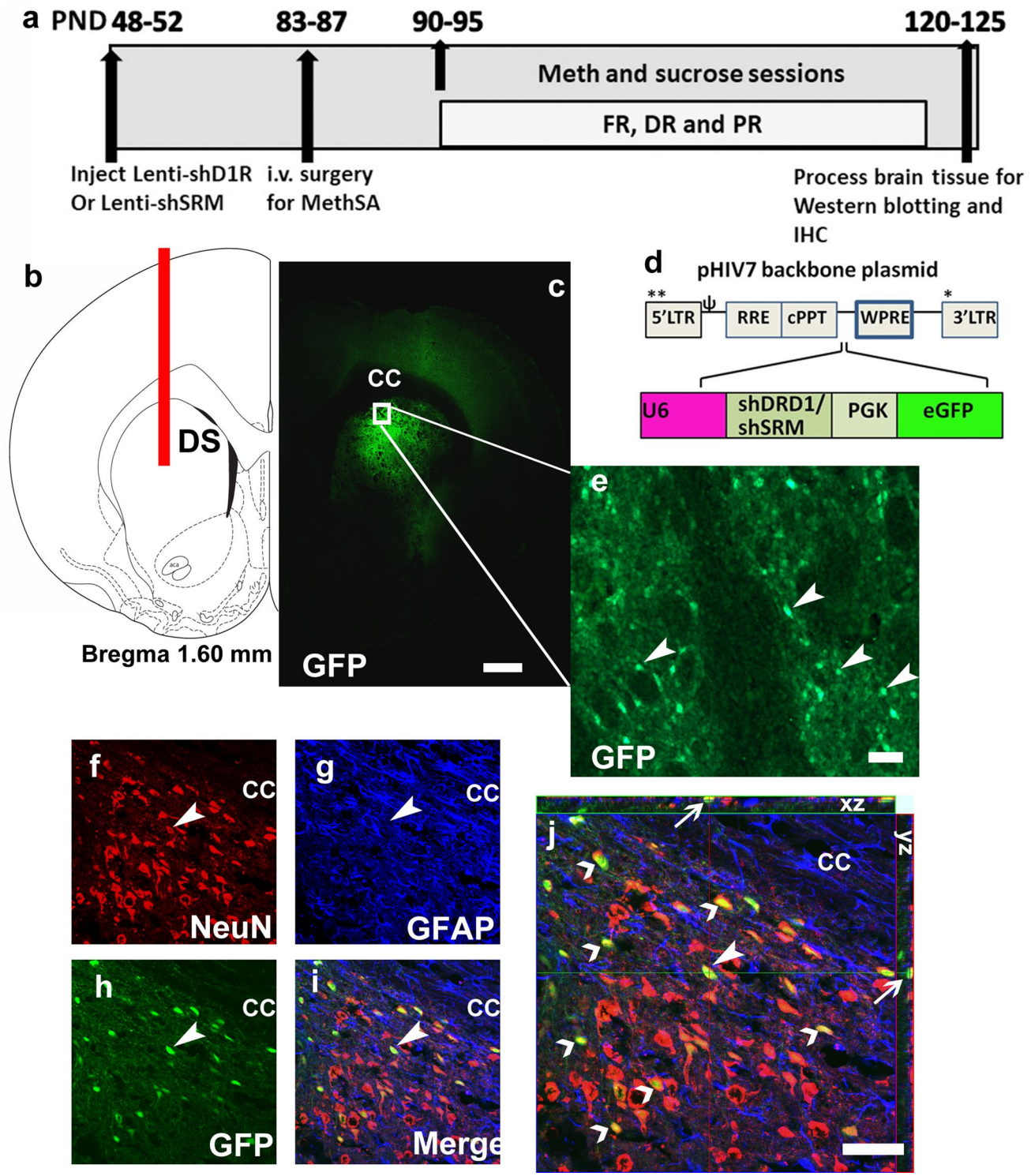

Brain tissue collection for immunohistochemistry and Western blotting

Tissue from a separate group of nine age-matched, virus and behavior-naïve rats was used for comparison in Western blotting analyses ('control' groups in Figs. 4 and 5, $n=5$ for methamphetamine analyses and $n=4$ for sucrose analyses). Rats (D1RshRNA and D1R-intact methamphetamine; D1RshRNA and D1R-intact sucrose; controls) were euthanized via rapid decapitation under light isoflurane anesthesia (3–5%) 1 h after conclusion of the PR session. The left hemisphere was snap frozen for Western blotting and the

◂**Fig. 1** **a** Schematic of the timeline of experimental design and corresponding age of rats (in postnatal days, PND) from the start to the completion of the study; *FR* fixed ratio, *DR* dose–response, *PR* progressive ratio. **b** Schematic representation of a coronal section through the dorsal striatum of the adult rat brain indicating the placement of injector needle for virus infusions. *DS* dorsal striatum. **c** Representative low-magnification image of the striatal tissue indicating endogenous GFP labeling in the brain. *cc* corpus callosum, *GFP* green fluorescent protein. **d** Schematic of the lentiviral vector backbone indicating the genes of interest along with the U6 promoter that are inserted upstream of the WPRE in the pHIV-7 vector; *eGFP* enhanced green fluorescent protein. **e** Subsection of DS from (**c**), with GFP-positive cells indicated by arrowheads. **f–i** Confocal triple labeling of NeuN (CY3, marker for neurons, **f**), GFAP (CY5, marker for astroglia, **g**), GFP (CY2, marker for lentivirus, **h**) and the composite of all three images (**i**). Arrowhead points to a NeuN + GFP + colabeled cells that do not express GFAP (**i**). **j** Confocal z-stack image of (**i**) in orthogonal view indicating colabeling of the cell in (**f–i**) pointed with an arrowhead. *xy*- and *yz*-axis is indicated in (**j**) with thin arrows to demonstrate equal penetration of GFP, NeuN and GFAP antibodies. Open arrowheads point to additional NeuN + GFP + cells that do not express GFAP. Scale bar in (**c**) is 300 µm, in **e–j** is 30 um

right hemisphere was post-fixed in 4% paraformaldehyde for immunohistochemistry.

Validation of virus infection

Brain tissue containing the right hemisphere was sliced in 40-µm sections along the coronal plane in a cryostat. A section from the injection site of the dorsal striatum was mounted on Superfrost® Plus slides and dried overnight and was visualized for expression of GFP under a fluorescent microscope (AxioImager A2). Rats from methamphetamine ($n = 4$) and sucrose ($n = 2$) groups were excluded from the study due to incorrect coordinates. Examination of striatal sections demonstrate robust GFP labeling confined to the dorsal striatum (Fig. 1c).

Immunohistochemistry and confocal microscopy

Sections were slide mounted and processed for neuronal marker neuronal nuclease (NeuN; mouse primary: 1:100; EMD Millipore, Billerica, MA, CY3 donkey anti-mouse secondary: 1:200), astroglial marker glial fibrillary acidic protein (GFAP; chicken primary: 1:500; Abcam, Cambridge, MA, CY5 donkey anti-chicken secondary: 1:200), and GFP (1:500; rabbit primary; ab6556; Abcam, Cambridge, MA, CY2 donkey anti-rabbit secondary 1:200). The sections were pretreated (Mandyam et al. 2004), blocked, and incubated with the primary antibodies followed by secondary antibodies and colabeling were assessed by confocal analysis. Confocal analysis of triple labeled cells in the dorsal striatum was performed with a Zeiss Axiovert 100 M and LSM510 using a previously published method (Kim and Mandyam 2014). Colocalization of antibodies was assessed with the confocal system by an analysis of adjacent *z*-sections (using gallery function and orthogonal function for equal penetration of the antibodies). Optical sectioning in the *z* plane was performed using multitrack scanning with an optimal section thickness of 0.5 µm. Confocal analysis was performed at 400×.

Western blotting

Tissue punches from 300-µm-thick sections of dorsal striatum (methamphetamine groups: controls, $n = 5$; D1-intact, $n = 10$; D1shRNA, $n = 11$; sucrose groups: controls, $n = 4$; D1-intact, $n = 10$; D1shRNA, $n = 8$) encompassing the injection site were homogenized on ice by sonication in MES buffer (150 mM NaCl, 2 mM EDTA and 150 mM Na_2CO_3, 1 mM EDTA with Protease Inhibitor Cocktail and Phosphatase Inhibitor Cocktails II and III diluted 1:100) heated at 70 °C for 10 mins, and stored at − 80 °C until determination of protein concentration by a detergent-compatible Lowry method (Bio-Rad, Hercules, CA, USA). Samples were mixed (1:1) with a Laemmli sample buffer containing β-mercaptoethanol. Protein samples (20 µg) were run on 10% SDS-PAGE gels (Bio-Rad, Hercules, CA, USA) and transferred to polyvinylidene fluoride membranes (PVDF pore size 0.2 µm). Membranes were blocked with 5% milk (w/v) in TBST (25 mM Tris–HCl (pH 7.4), 150 mM NaCl and 0.1% Tween 20 (v/v)) for 2–4 h at room temperature and were incubated with the primary antibody for 16–20 h at 4 °C: antibody for D1R (1:1000, Abcam AB20066), dopamine D2 receptors (D2R, 1:500, Sigma Aldrich AB5084P), Cav-1 (1:500, Cell Signaling D46G3), PSD 95 (1:1000, Invitrogen MA1-045), MAPK-1 (1: 1000, Cell Signaling 137F5), flotillin-1 (1:1000, ProteinTech 15571–1-AP), and DAT (1:1000, Santa Cruz sc-32258). Membranes were then washed with TBST and incubated for 1 h at room temperature with horseradish peroxide-conjugated goat antibody to rabbit (1:1000 for D1R, D2R, Cav-1 and flotillin-1, 1:200 for MAPK-1) or horseradish peroxide-conjugated goat antibody to mouse (1:1000 for PSD-95) or horseradish peroxide-conjugated goat antibody to rat (1:1000 for DAT) in TBST. Following subsequent washes, immunoreactivity was detected using SuperSignalWest Dura chemiluminescence detection reagent (Thermo Scientific) and images were collected using a digital imaging system (Azure Imager c600). For normalization purposes, membranes were incubated with 0.125% coomassie stain for 5 min and washed three times for 5–10 min in destain solution. Densitometry was performed using ImageJ software (NIH). The signal value of the band of interest following subtraction of the background calculation was then expressed as a ratio of the corresponding Coomassie signal (following background subtraction). This ratio of expression for each band was then expressed as a percent of the drug- and behavior-naïve control rat included on the same membrane (Fig. 4).

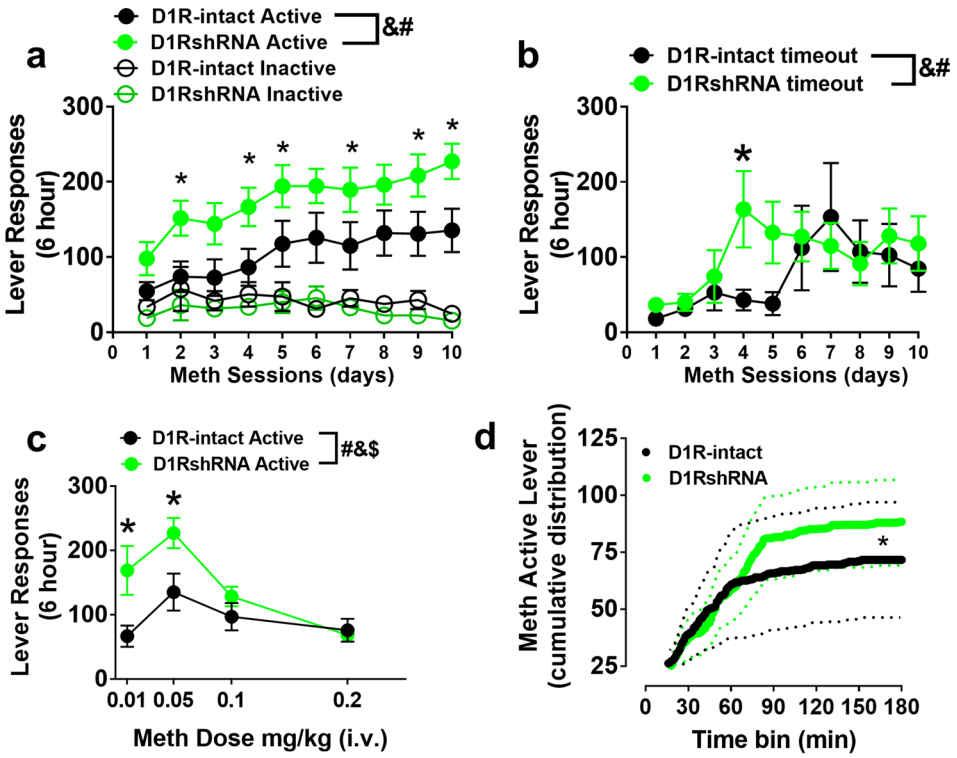

Fig. 2 **a** Active and inactive lever responses during extended 6-h access sessions of methamphetamine self-administration. **b** Active lever responses during timeout period. **c** Active lever responses during dose–response sessions. **d** Cumulative active lever responding across progressive-ratio sessions. $n = 11$ D1RshRNA and $n = 10$ D1R-intact rats. Solid line is the average cumulative response and dotted lines are ± SEM. $^{*}p < 0.05$ vs. D1R-intact rats by repeated measures ANOVA. $^{\&}p < 0.05$, significant group × session (**a**, **b**), or group × dose (**c**) interaction; $^{\#}p < 0.05$, significant main effect of session or dose; $^{\$}p < 0.05$, significant main effect of treatment by repeated measures ANOVA

Sucrose density gradient fractionation

Lysate (0.5 µg/ml of protein in 1 ml) was prepared to be added to the sucrose gradient (methamphetamine groups: controls, $n = 4$; D1-intact, $n = 4$ and D1shRNA, $n = 4$). Sucrose gradient was made with MES-buffered saline (MBS), where sucrose was added to different volumes of the buffer to create initial 5%, 35%, and 80% concentration of sucrose solutions. In a 12-ml centrifuge tube, 1 ml of 80% sucrose was mixed with 1 ml of homogenate to create a 40% sucrose solution. 6 ml of 35% sucrose was floated onto the resulting 40% sucrose layer. Finally, 4 ml of 5% sucrose was floated onto the 35% sucrose layer. A SW41Ti rotor (Beckman Coulter, Fullerton, California, USA) set to 4 °C was utilized to centrifuge samples for 18 h at 39,000 rpm. Gradients were aliquoted by every 1 ml from top to bottom of the centrifuge tube, represented fractions 1–12 of the sucrose density gradient and fractions 3–6 (buoyant/lipid raft rich) and 9–12 (heavy) were prepared for Western blotting. Samples (40 µl per fraction) were mixed with a 5 × Laemmli sample buffer and were run on 10% SDS-PAGE gels (Bio-Rad) and transferred to polyvinylidene fluoride membranes (PVDF). Membranes were blocked with 5% milk (w/v) in TBST for 2–4 h at room temperature and were incubated with the primary antibody for 16–20 h at 4 °C: antibody for D1R, Cav-1, PSD 95, MAPK-1, flotillin-1 and DAT. Blots were then washed with TBST and incubated for 1 h at room temperature with horseradish peroxide-conjugated goat antibody to rabbit or horseradish peroxide-conjugated goat antibody to mouse in TBST. Following subsequent washes, immunoreactivity was detected using SuperSignalWest Dura chemiluminescence detection reagent (Thermo Scientific) and images were collected using a digital imaging system (Azure Imager c600). Densitometry was performed using ImageJ software (NIH). The signal value of the band of interest following subtraction of the background calculation was then expressed and used for statistical analysis.

Statistical analyses

The methamphetamine and sucrose self-administration data are expressed as the average total number of lever responses per session. Methamphetamine or sucrose self-administration during the 6-h FR maintenance and dose–response sessions was examined using a two-way repeated-measures analysis of variance (ANOVA) followed by the uncorrected Fisher's LSD post hoc test. For maintenance sessions, active and inactive lever presses were analyzed separately (Fig. 1a). Independent samples *t* tests were used to determine group differences in total methamphetamine/sucrose deliveries earned per PR session (Fig. 3c). The cumulative frequency distributions for responding under the PR schedule (Figs. 2d, 3d) were compared between the D1R-intact and D1RshRNA groups using the two-sample Kolmogorov–Smirnov test for equality of continuous probability distributions. Significance was assessed at $\alpha = 0.05$. A one-way ANOVA was conducted

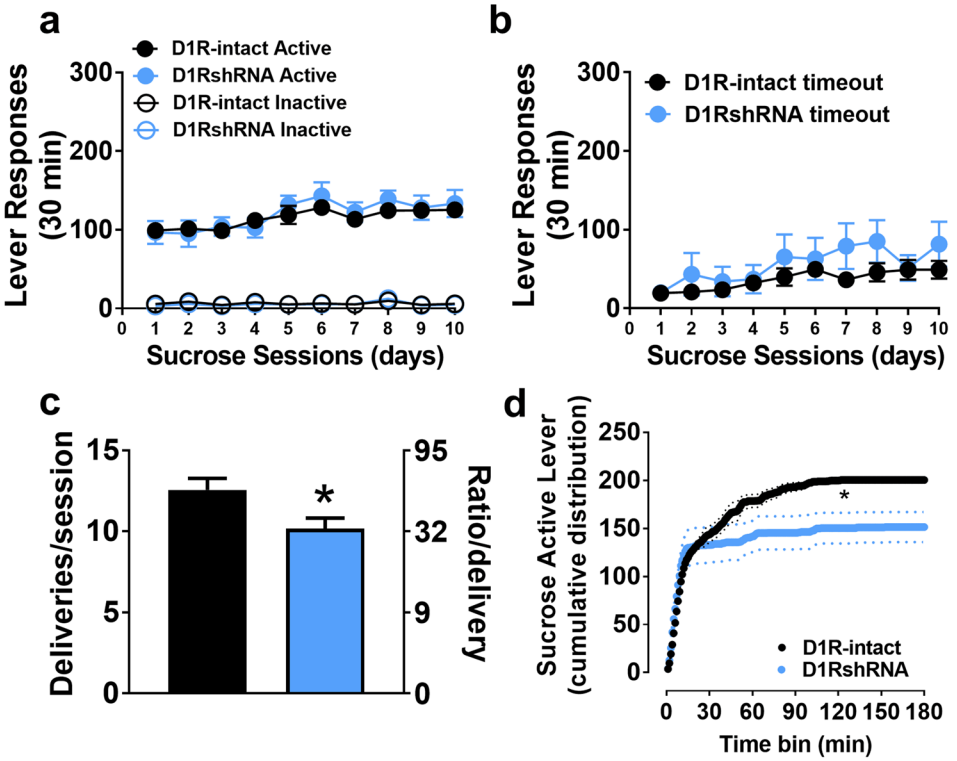

Fig. 3 **a** Active and inactive lever responses during 30 min sucrose self-administration sessions. **b** Active lever responses during timeout period. **c** Average number of sucrose deliveries earned per progressive-ratio session with corresponding number of required lever presses. **d** Cumulative active lever responding across progressive-ratio sessions. $n = 8$ D1RshRNA and $n = 8$ D1R-intact rats. Solid line is the average cumulative responses and dotted lines are ± SEM. *$p < 0.05$ vs. D1R-intact rats overall

to determine differences between drug- and behavior-naïve controls, D1R-intact, and D1RshRNA rats for Western blots of all proteins followed by Tukey's post hoc tests for each protein. Western blot analysis was conducted on percent change values from age-matched-naive controls (Fig. 4b, d). Data are expressed as mean ± SEM in all graphs.

Results

Effect of D1R silencing on methamphetamine self-administration

Methamphetamine self-administration behavior (FR, DR and PR sessions) did not differ between the shSRM-RNA rats and those that were virus naïve. Therefore, the rats from both these groups were combined and is indicated as the D1R-intact group ($n = 10$, Fig. 2).

FR Two-way ANOVA of active lever responses did not detect a significant session × treatment interaction. However, there was a significant main effect of session ($F(9,171) = 9.17$, $p < 0.0001$) and treatment ($F(1,19) = 5.43$, $p = 0.03$; Fig. 2a). All rats increased the number of active lever presses across the ten acquisition sessions, but D1RshRNA rats also showed a higher number of active lever presses on day 2 (~ 152) vs day 1 (~ 98), whereas active lever presses in D1R-intact rats did not increase significantly until day 5 (~ 118) compared to day 1 (~ 55, ps < 0.05; Fig. 2a). D1RshRNA and D1R-intact rats did not differ in inactive lever presses [treatment: $F(1,19) = 0.84$, $p > 0.05$], nor did inactive presses change across the acquisition phase [session: $F(9,171) = 1.31$, $p > 0.05$; Fig. 2a]. Two-way ANOVA of timeout lever responses detected a significant session × treatment interaction ($F(9,171) = 2.06$, $p = 0.03$), a significant main effect of sessions ($F(9,171) = 4.76$, $p < 0.0001$) and did not detect a main effect of treatment ($F(1,19) = 0.5$, $p = 0.47$; Fig. 2b). Post hoc analysis demonstrated higher number of responses on day 4 in D1RshRNA rats compared to D1R-intact rats (Fig. 2b).

Dose–response There was a significant main effect of dose ($F(3,57) = 12.94$, $p < 0.0001$) and main effect of treatment ($F(1,19) = 5.07$, $p = 0.03$; Fig. 2c). A treatment × dose interaction [$F(3,57) = 4.271$, $p < 0.01$] reflected that D1RshRNA rats pressed the active lever more than D1R-intact rats at lower doses of meth (0.01 and 0.05 mg/kg) but did not differ when responding for higher doses (0.1 and 0.2 mg/kg; Fig. 2c). Treatment groups did not differ in the number of inactive nor timeout lever presses at any dose (not shown).

PR D1RshRNA rats did not significantly differ from D1R-intact rats (10.4 ± 1.4 vs. 8.7 ± 1.7; ($t(19) = 0.78$, $p > 0.05$) in infusions earned. Further analysis of active lever responses revealed significant group differences in the cumulative reinforced responses (Kolmogorov–Smirnov $D = 0.594$, $p < 0.001$; Fig. 2d), in which the D1R-intact rats exhibited lower responding plateaus than D1RshRNA rats.

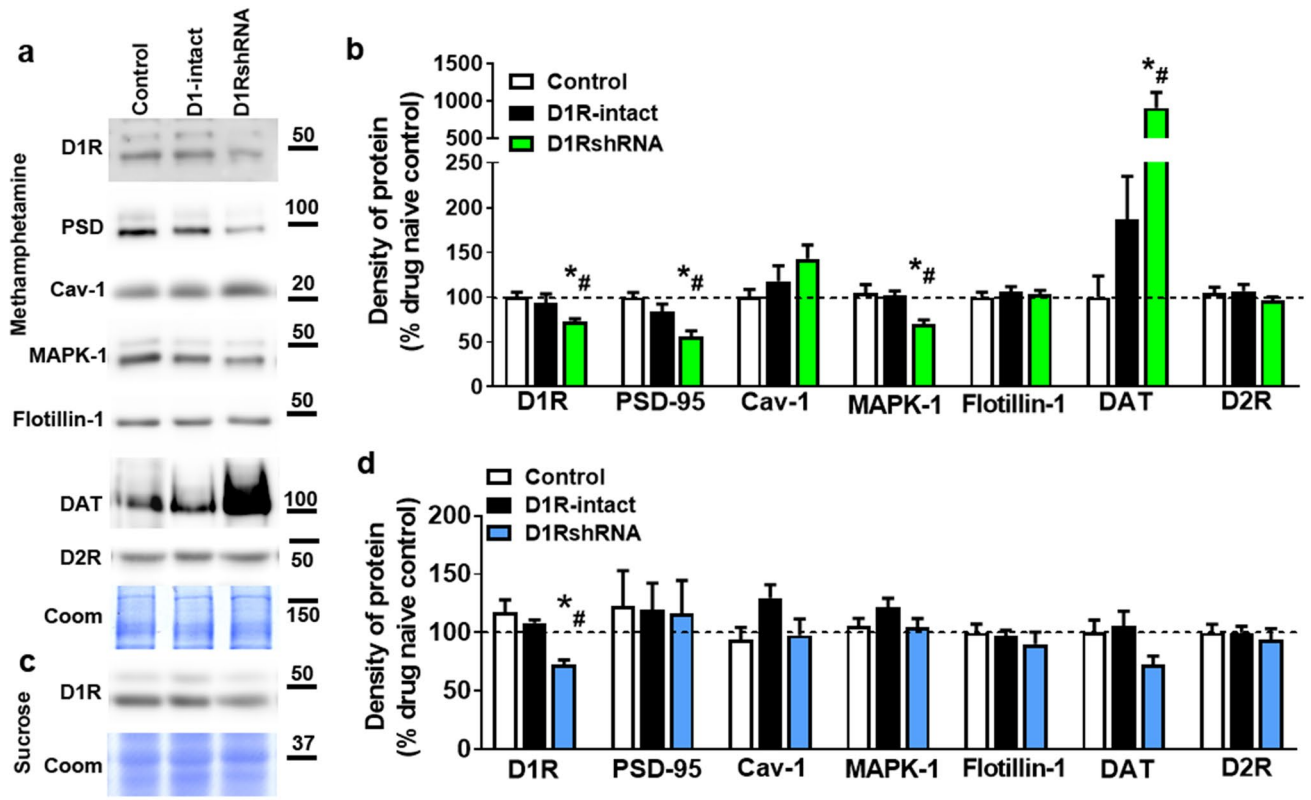

Fig. 4 **a** Representative immunoblots of the various proteins used for Western blotting analysis from methamphetamine and control rats. Molecular masses (kilodaltons) are indicated adjacent to each representative blot. Corresponding Coomassie staining (Coom) of the membrane is shown as loading control. Quantitative analysis of protein expression in tissue from methamphetamine-exposed (**b**) and sucrose-exposed (**d**) rats as well as behavior- and virus-naïve controls (white bars in b and d). **c** Representative immunoblot of D1R from sucrose and control rats. Molecular mass (kilodaltons) is indicated adjacent to the blot. Corresponding Coomassie staining (Coom) of the membrane is shown as loading control. $^{*}p<0.05$ vs. controls, $^{\#}p<0.05$ vs. D1R-intact rats by one-way ANOVA followed by post hoc analysis. $n=4$–11 in each group

Effect of D1R silencing on sucrose self-administration

Sucrose self-administration behavior (FR and PR sessions) did not differ between the shSRM-RNA rats and those that were virus naïve. Therefore the rats from both these groups were combined and are indicated as D1R-intact group ($n=12$, Fig. 3).

FR Both groups discriminated the active vs. inactive lever across each of the ten sucrose self-administration sessions (paired *T* tests, ps < 0.0001), and D1RshRNA and D1R-intact rats did not differ in the number of active [treatment: $F(1,18)=0.125$, $p>0.05$], nor inactive [treatment: $F(1,18)=0.234$, $p>0.05$] lever presses (Fig. 3a). Both groups showed similarly increased responding for sucrose on day 5 (~ 125 presses), and every day thereafter, compared to day 1 (~ 100 presses, session: $F(9,162)=12.06$, $p<0.05$; Fig. 3a). Timeout responding similarly increased across the ten sucrose self-administration sessions in both groups, from ~ 19 lever presses on day 1 to ~ 57 lever presses on day 10 (Fig. 3b; treatment, and session × treatment: ps > 0.05).

PR On average, D1RshRNA rats earned 10.2 sucrose deliveries during the PR session and was significantly fewer than D1R-intact rats (12.6 deliveries; $(t(13)=2.33$, $p<0.05)$ (Fig. 3c). Further analysis of active lever responses revealed significant group differences in the cumulative distributions (Kolmogorov–Smirnov $D=0.8$, $p<0.0001$; Fig. 2d), in which the D1R-intact group exhibited higher responding plateaus for the sucrose reinforcer compared with the D1RshRNA group.

Expression of D1R, D2R, DAT and proteins associated with D1R signaling in dorsal striatum tissue homogenates

Methamphetamine rats Treatment effects by one-way ANOVA reflected that, compared to methamphetamine-naïve/age-matched controls, methamphetamine-exposed D1R-intact rats showed similar expression levels of D1R,

D2R, PSD-95, Cav-1, MAPK-1, flotillin-1 and DAT (Group ps > 0.05, Fig. 4ab). However, D1RshRNA rats showed reduced expression of D1R [$F(2,23) = 5.6$], PSD-95 [$F(2,23) = 11.4$] and MAPK-1 [$F(2,23) = 9.6$], and enhanced expression of DAT [$F(2,23) = 5.4$] compared to controls and D1-intact rats by one-way ANOVA (ps < 0.05; Fig. 4ab). D2Rs were unaltered in D1RshRNA rats vs. controls ($p = 0.33$).

Sucrose rats D1RshRNA, D1R-intact, and sucrose-naïve, age-matched control rats did not differ from each other in expression of D2R (0.80), PSD-95 ($p = 0.98$), Cav-1 ($p = 0.12$), MAPK-1 ($p = 0.24$), flotillin-1 ($p = 0.66$) and DAT ($p = 0.07$) by one-way ANOVA (Fig. 4c, d). However, a treatment effect [$F(2,19) = 7.79$, $p < 0.01$] reflected that D1RshRNA rats showed reduced D1R expression compared to both D1R-intact and -naïve controls (ps < 0.05), which did not differ from each other (Fig. 4d).

Expression of D1R, DAT and proteins associated with D1R signaling in sucrose density gradient fractionation of dorsal striatum tissue

To determine the subcellular localization of D1Rs, DAT and proteins associated with D1R signaling, we carried out discontinuous sucrose density gradient fractionation of DS tissue. This method has been used to isolate membrane subdomains (fractions 3–6 and 9–10) that have distinct biochemical compositions or properties, such as lipid rafts [buoyant fractions 3–6 and heavy fractions 9–12; (Voulalas et al. 2011; Mandyam et al. 2015)]. Two-way ANOVA was performed with sucrose fractions as within subject and treatment groups as between subject factors. In control rats, we found greater proportion of D1Rs in heavy fractions compared to buoyant fractions (Fig. 5a, b), where PSD-95, MAPK-1, flotillin-1, Cav-1 and DAT (Fig. 5c–l) were also observed. Two-way ANOVA of D1R expression demonstrated a significant fraction × treatment interaction ($F(14,63) = 1.954$, $p < 0.05$) and main effect of fraction ($F(7,63) = 535.9$, $p < 0.05$). Post hoc analysis showed higher levels of D1R in D1R-intact and D1RshRNA rats compared to controls in fraction 12 and lower levels of D1R in D1R-intact and D1RshRNA rats compared to controls in fraction 11 ($ps < 0.05$). Two-way ANOVA of PSD-95 expression demonstrated a significant fraction × treatment interaction $F(14,63) = 16.68$, $p < 0.01$ and main effect of fraction $F(7,63) = 123.5$, $p < 0.01$. Post hoc analysis showed significant relocation of PSD-95 from heavy fractions to buoyant fractions in D1-intact rats compared with controls and D1shRNA rats ($ps < 0.05$). Two-way ANOVA of Cav-1 expression demonstrated a significant fraction × treatment interaction $F(14,63) = 22.05$, $p < 0.001$ and main effect of fraction $F(7,63) = 92.6$, $p < 0.001$. Post hoc analysis showed higher levels of Cav-1 in D1R-intact and D1RshRNA rats compared to controls in buoyant fractions, and lower levels of Cav-1 in D1R-intact and D1RshRNA rats in heavy fractions compared to controls ($ps < 0.01$). Two-way ANOVA of MAPK-1 expression demonstrated a significant fraction × treatment interaction $F(14,63) = 3.53$, $p < 0.01$ and main effect of fraction $F(7,63) = 294.4$, $p < 0.001$. Post hoc analysis showed higher levels of MAPK-1 in D1R-intact and D1RshRNA rats compared to controls in fraction 12 and lower levels of MAPK-1 in D1R-intact and D1RshRNA rats compared to controls in fraction 11 ($ps < 0.05$). Post hoc analysis also showed significant relocation of MAPK-1 from heavy fractions to buoyant fractions in D1-intact rats compared with controls ($ps < 0.05$). Two-way ANOVA of flotillin-1 expression demonstrated a significant fraction × treatment interaction $F(14,63) = 7.1$, $p < 0.001$ and main effect of fraction $F(7,63) = 42.1$, $p < 0.001$. Post hoc analysis showed higher levels of flotillin-1 in D1R-intact rats compared to controls in buoyant fractions and lower levels of flotillin-1 in D1R-intact and D1RshRNA rats in heavy fractions compared to controls (ps < 0.05). Two-way ANOVA of DAT expression demonstrated a significant fraction × treatment interaction $F(14,63) = 2.3$, $p < 0.01$ and main effect of fraction $F(7,63) = 109.4$, $p < 0.001$. Post hoc analysis showed higher levels of DAT in D1R-intact and D1RshRNA rat compared to controls in fraction 12 and lower levels of DAT in D1R-intact and D1RshRNA rats compared to controls in fraction 11 (ps < 0.05).

Discussion

In this study, we describe the effect of reducing levels of D1Rs in the DS via RNA interference on methamphetamine addiction-like behaviors. D1RshRNA rats show a 30% decrease in D1R protein expression in the DS. D1RshRNA rats did not show any changes in D2R levels. A striking observation was that D1RshRNA rats demonstrated a higher rate of responding during extended access sessions, greater intake of methamphetamine across doses, and willingness to work harder to obtain the drug compared to their D1R-intact counterparts. This behavioral profile is associated with altered expression of DAT and plasticity-related proteins regulating D1R function, including MAPK-1 and PSD-95 in the DS. These changes support altered mesencephalic dopaminergic transmission, and that they are not accompanied by differential subcellular localization of D1Rs, DAT, MAPK-1, PSD-95, Cav-1 and flotillin-1. These results indicate that individuals with reduced D1R expression in the DS will be more vulnerable to drug addiction.

Lentiviral-mediated application of targeted mRNA and proteins is a commonly used tool in behavioral neuroscience because it provides genetic control with minimal observed anatomical nor behavioral side effects in adult rats (Johnson

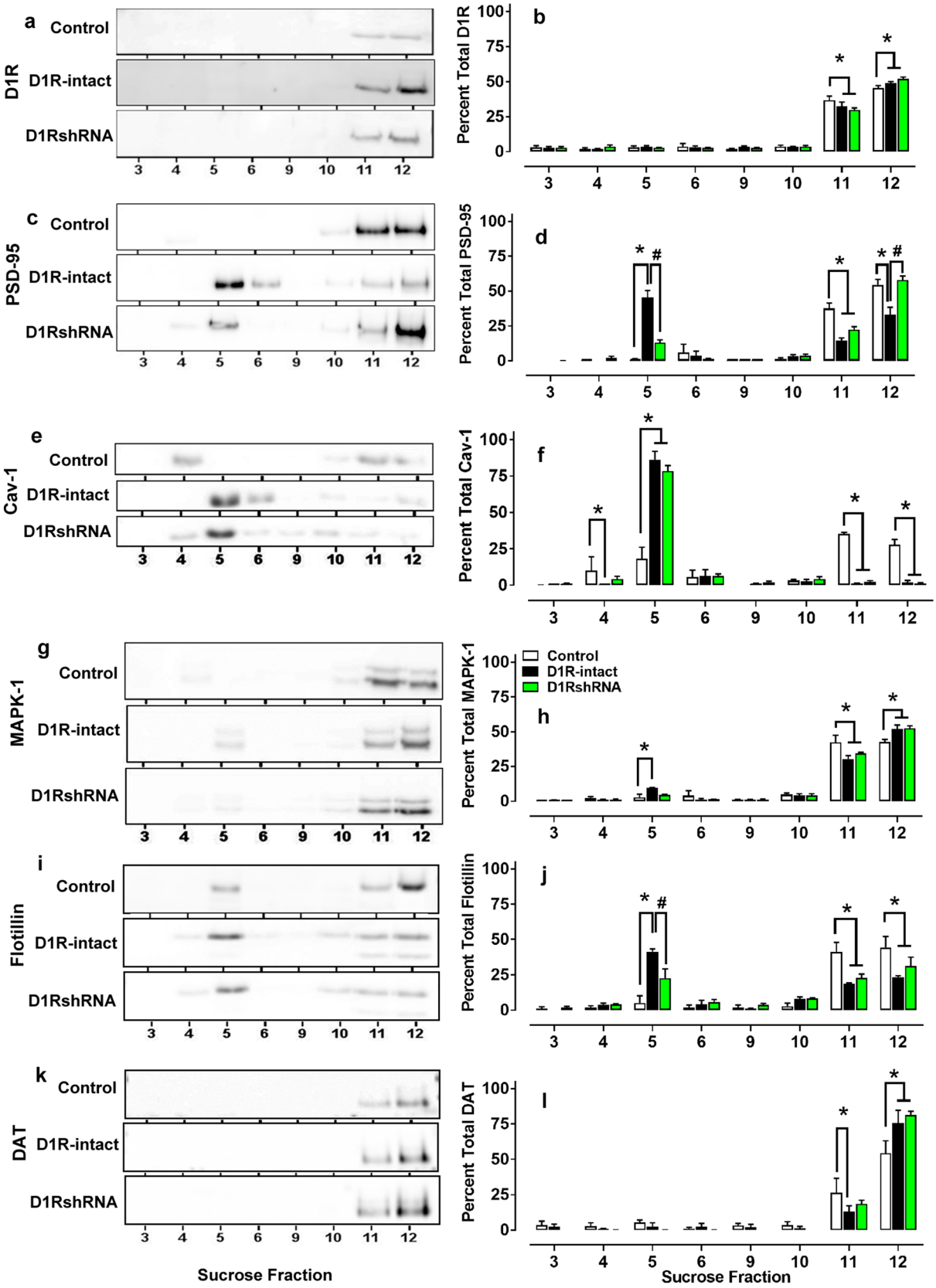
a
Control
D1R-intact
D1RshRNA
D1R
3 4 5 6 9 10 11 12
b
Percent Total D1R
100
75
50
25
0
c
PSD-95
d
Percent Total PSD-95
e
Cav-1
f
Percent Total Cav-1
g
MAPK-1
h
Percent Total MAPK-1
Control
D1R-intact
D1RshRNA
i
Flotillin
j
Percent Total Flotillin
k
DAT
l
Percent Total DAT
Sucrose Fraction

◂**Fig. 5** Representative immunoblots (**a**, **c**, **e**, **g**, **i**, **k**) and quantitative analysis (**b**, **d**, **f**, **h**, **j**, **l**) of the various proteins used for sucrose density gradient fractionation analysis from methamphetamine and behavior- and virus-naïve control rats. $^{*}p<0.05$ vs. controls, $^{\#}p<0.05$ vs. D1R-intact rats by ANOVA followed by post hoc analysis. $n=4$ in each group

and Kenny 2010; Yin et al. 2017; Gao et al. 2019; Oliver et al. 2019; Shen et al. 2019). D1RshRNA animals were tested for methamphetamine self-administration and sucrose self-administration. Rats that self-administered sucrose were considered behavioral control groups since sucrose is a non-drug reinforcer commonly used to determine the specificity of behavioral effects (Noonan et al. 2010; Galinato et al. 2018a, b; Jaramillo et al. 2018; Kruyer et al. 2019; Vazquez et al. 2019; Turner et al. 2020). Accordingly, operant self-administration of sucrose does not alter the expression of the proteins studied in our report, and we propose that the sucrose group represents the pure effect of D1RshRNA to be compared with the effect of D1RshRNA with methamphetamine self-administration. A potential limitation in the interpretation of these findings is that D1RshRNA may have non-specific effects, including in non-D1R containing cells. However, we believe that these studies are beyond the scope of the current study.

While results demonstrated that D1RshRNA rats had increased responding for methamphetamine, D1RshRNA rats showed similar responding for sucrose in FR sessions compared with D1R-intact rats. However, our results indicate that D1RshRNA rats have a reduced propensity to lever press for sucrose reward in PR sessions. Therefore, D1RshRNA rats showed reduced motivation to seek sucrose or obtain food reward, supporting previous studies that were conducted with D1R antagonists (Wise 2006). A reduction in PR responding for sucrose in D1RshRNA rats suggests that D1Rs might distinctly be promoting the rewarding properties of sucrose. However, the lack of an effect on FR responding for sucrose suggests that there is an interaction between type of reinforcer (drug vs. natural reward), operant requirement (FR vs. PR) and D1R's role in reward value. This three-way relationship warrants further study. Interestingly, despite relatively high levels of FR responding for sucrose, this behavioral profile does not seem to be due to altered expression of plasticity-related proteins associated with D1R signaling in the DS. This lack of an effect is consistent with the failure of sucrose self-administration to increase striatal D1R expression (Bello et al. 2002; Tonissaar et al. 2006; Rospond et al. 2019), together suggesting that repeated sucrose self-administration is not sufficient to alter D1R signaling. However, it should be noted that sucrose access was limited to 30 min per day, and emerging evidence suggests that more extended (24 h), vs. shorter (30 min) access to sucrose produces distinct profiles of motivated behavior (Kreisler et al. 2017, 2018). Nevertheless, it appears that D1RshRNA rats have a reduction in motivation to work for the specific natural reward tested here.

Brain region-specific targeting of D1R using antagonists reveal a critical positive role for striatal and amygdalar D1Rs in promoting the rewarding properties of several drugs of abuse including opiates, nicotine, alcohol, and psychostimulants (Shippenberg et al. 1993; Abrahams et al. 1998; Berglind et al. 2006; Fenu et al. 2006; Spina et al. 2006; Chaudhri et al. 2009; Liu et al. 2011; Young et al. 2014). However fewer studies have utilized site-specific genetic down-regulation of D1R function, a less invasive approach offering more temporally consistent and more specific, and quantifiable loss-of-function on a whole-cell basis (Noori-Daloii et al. 2012). The few that have taken this approach confirm the importance of ventral striatal D1R expression in rewarding properties of alcohol (Bahi and Dreyer 2012). To our knowledge, our study is the first to use the shRNA approach to specifically reduce D1R expression in the DS to study its role in methamphetamine addiction.

However, our results might seem inconsistent with previous studies conducted with D1R antagonists administered systemically (Bardo et al. 1999; Brennan et al. 2009; Gong et al. 2016), in that D1R knockdown in the DS increased FR responding for methamphetamine during extended access sessions, and interpreted as a sensitization to acquisition of escalated methamphetamine taking. One explanation for this finding may be the previously described DR compensatory response, in which downregulation of DR function produces subsequent hypersensitivity to dopaminergic stimulation (Rupniak et al. 1986). Perhaps D1RshRNA treatment led to hypersensitivity of existing D1Rs, leading to increased sensitivity to methamphetamine's agonistic effects on dopaminergic transmission and, consequently, increased rewarding properties of methamphetamine. An additional explanation might lie in the controversial interpretation of FR1 responding as a measure of reinforcing efficacy of drugs of abuse. While relative increases in FR1 responding are often interpreted as increased reward value of the reinforcer, classical studies using manipulation of mesolimbic dopamine signaling provide support for the interpretation that such an increase in rate of responding is a compensatory response to a decrease in reinforcing efficacy (Roberts et al. 1989; Roberts 1993; Richardson and Roberts 1996; Morgan et al. 2002). PR paradigms circumvent this interpretational dilemma since they are more sensitive to responding (rather than just consumption), and, moreover, can assess the *magnitude* of reinforcer efficacy by incrementally increasing response requirements. Indeed, PR breakpoint (lever pressing requirement at which a subject no longer responds for the reinforcer) is more reliably sensitive to drug dose (Richardson and Roberts 1996). Therefore, in

the current study, increased FR responding, a vertical shift in dose–response curve and increased PR responding in D1shRNA rats could be interpreted as enhanced reinforcing efficacy of methamphetamine and drug-vulnerable phenotype after striatal D1R knockdown compared to D1R-intact rats (Piazza et al. 1989, 2000).

The in vivo role of DAT (located presynaptically) and signaling molecules associated with D1Rs (located postsynaptically) in the context of methamphetamine addiction and motivated behavior has been minimally investigated (Baucum et al. 2004; Mizoguchi et al. 2004; Salahpour et al. 2008; Schwendt et al. 2009; Cremona et al. 2011; Shi and McGinty 2011; Cagniard et al. 2014). Our results reveal robust increases in the expression of DAT, and significant decreases in the activity MAPK-1 and expression of PSD-95 in D1RshRNA rats, and these effects correlated with increased vulnerability to methamphetamine addiction. Previous reports have correlated methamphetamine-induced enhanced striatal DAT expression to methamphetamine-induced neurotoxicity (Baucum et al. 2004). Notably, enhanced DAT expression is associated with hypodopaminergia in the DS (Giros et al. 1996; Salahpour et al. 2008), and this mechanism could explain the enhanced methamphetamine addiction-like behavior in D1RshRNA rats, i.e., a compensatory behavioral response due to reduced reward efficacy of methamphetamine (Spielewoy et al. 2001; Baucum et al. 2004; Salahpour et al. 2008; Ghisi et al. 2009; Xi et al. 2009; Cagniard et al. 2014). Whether D1Rs expressed by postsynaptic neurons are directly capable of inducing presynaptic alterations in DAT in the DS is unknown, and will be an important future pursuit. In addition, the presently observed hypoactivity of MAPK-1 and reduced expression of PSD-95 in D1RshRNA rats could be interpreted as a mechanism to compensate for the hypodopaminergic state, and lend support to this mechanistic hypothesis (Lindgren et al. 2002; Yao et al. 2004).

In the context of the above mechanism, subcellular localization of DR and DAT within lipid rafts may have relevance to the signaling and modulation of synaptic dopamine. For example, temporal and spatial regulation of signal transduction of D1Rs is provided by the lipid raft protein Cav-1 (Allen et al. 2007; Kong et al. 2007; Voulalas et al. 2011; Stary et al. 2012), and expression and endocytosis of DAT is regulated by the lipid raft protein flotillin-1 (Cremona et al. 2011). Our findings support previous studies from adult rodent brain samples to show that Cav-1 and flotillin-1 are localized in buoyant (lipid raft) and heavy (non-lipid raft) fractions, and D1Rs and DAT are predominantly localized to heavy fractions (Kang et al. 2006; Cremona et al. 2011; Voulalas et al. 2011). More notable is that methamphetamine self-administration did not alter the subcellular localization of D1Rs or DAT, indicating that the striatal alterations in expression, and not subcellular localization of these proteins predicted the enhanced vulnerability to methamphetamine addiction.

Next, mechanistic studies conducted in vitro in non-neuronal cells demonstrate that Cav-1 gene and protein expression are regulated by MAPK-1 activity (Engelman et al. 1999; Cohen et al. 2003), suggesting that Cav-1 can act as an inhibitor of signaling cascades involving MAPK-1 (Engelman et al. 1998; Galbiati et al. 1998). Accordingly, we demonstrate that although total expression of Cav-1 was not enhanced in D1RshRNA rats, there was a significant increase in Cav-1 expression in the buoyant fractions in D1RshRNA rats. Although the relocation of Cav-1 to buoyant fractions was predicted as an inverse effect of reduced MAPK-1 activity in D1RshRNA rats, the relocation of Cav-1 was also seen in D1R-intact rats. Relocation of Cav-1 to buoyant fractions occurred concurrently with relocation of PSD-95 and flotillin-1 to buoyant fractions. This suggests that self-administration of methamphetamine per se produced postsynaptic adaptations in the DS. Such adaptations may include more stable scaffolds, creating subdomains within the plasma membrane, which could promote a microenvironment for compromised D1R signaling. Taken together, findings from D1RshRNA rats indicate that enhanced vulnerability to methamphetamine addiction is predicted by dysfunctional dopamine signaling coupled with altered neuronal membrane microdomains in the DS.

In conclusion, results of the present study suggest a role for D1Rs in the DS that is unique to methamphetamine addiction-like behavior and indicate potential intracellular molecular targets that might play a role in synaptic changes that accompany these behavioral changes. A minor limitation is that the current study was conducted in male subjects. Given the increasing number of studies that highlight the importance of including sex as a biological variable in exploring neuroplasticity changes that predict addiction-like behaviors (Lynch 2006; Becker 2016; Becker et al. 2017; Song et al. 2018; Becker and Chartoff 2019), the current findings in male rats may not be extendable to female subjects. Therefore, future studies should continue to outline the mechanistic relationships between D1Rs, DAT and signaling molecules in the context of compulsive methamphetamine self-administration in male and female subjects.

Acknowledgements Funds from the Department of Veterans Affairs (BX003304 to CDM), National Institute on Drug Abuse and National Institute on Alcoholism and Alcohol Abuse (AA020098 and DA034140 to CDM) and start-up funds from VMRF (to CDM) supported the study. The authors thank Dr. Atsushi Miyanohara, Director, UCSD viral vector core, for his assistance with plasmid generation and virus production. The authors thank McKenzie Fannon for assistance with animal surgeries, animal behavior and tissue processing, and Wulfran Trenet and Rocio Erandi Heyer Osorno for immunohistochemistry and Western blotting analysis. A significant proportion of this work was submitted in part as Master's Thesis by M.J.T. to the Division of Biological Sciences, University of California, San Diego.

Compliance with ethical standards

Conflict of interest The authors declare no conflict of interest. The funders had no role in the design of the study; in the collection, analyses, or interpretation of data; in the writing of the manuscript, and in the decision to publish the results.

References

Abrahams BS, Rutherford JD, Mallet PE, Beninger RJ (1998) Place conditioning with the dopamine D1-like receptor agonist SKF 82958 but not SKF 81297 or SKF 77434. Eur J Pharmacol 343:111–118

Ahmed SH, Koob GF (2004) Changes in response to a dopamine receptor antagonist in rats with escalating cocaine intake. Psychopharmacology 172:450–454

Allen JA, Halverson-Tamboli RA, Rasenick MM (2007) Lipid raft microdomains and neurotransmitter signalling. Nat Rev Neurosci 8:128–140

Bahi A, Dreyer JL (2012) Involvement of nucleus accumbens dopamine D1 receptors in ethanol drinking, ethanol-induced conditioned place preference, and ethanol-induced psychomotor sensitization in mice. Psychopharmacology 222:141–153

Bai J, Blot K, Tzavara E, Nosten-Bertrand M, Giros B, Otani S (2014) Inhibition of dopamine transporter activity impairs synaptic depression in rat prefrontal cortex through over-stimulation of D1 receptors. Cereb Cortex 24:945–955

Bardo MT, Valone JM, Bevins RA (1999) Locomotion and conditioned place preference produced by acute intravenous amphetamine: role of dopamine receptors and individual differences in amphetamine self-administration. Psychopharmacology 143:39–46

Baucum AJ, Rau KS, Riddle EL, Hanson GR, Fleckenstein AE (2004) Methamphetamine increases dopamine transporter higher molecular weight complex formation via a dopamine- and hyperthermia-associated mechanism. J Neurosci 24:3436–3443

Becker JB (2016) Sex differences in addiction. Dialogues Clin Neurosci 18:395–402

Becker JB, Chartoff E (2019) Sex differences in neural mechanisms mediating reward and addiction. Neuropsychopharmacology 44:166–183

Becker JB, McClellan ML, Reed BG (2017) Sex differences, gender and addiction. J Neurosci Res 95:136–147

Bello NT, Lucas LR, Hajnal A (2002) Repeated sucrose access influences dopamine D2 receptor density in the striatum. NeuroReport 13:1575–1578

Berglind WJ, Case JM, Parker MP, Fuchs RA, See RE (2006) Dopamine D1 or D2 receptor antagonism within the basolateral amygdala differentially alters the acquisition of cocaine-cue associations necessary for cue-induced reinstatement of cocaine-seeking. Neuroscience 137:699–706

Brennan KA, Carati C, Lea RA, Fitzmaurice PS, Schenk S (2009) Effect of D1-like and D2-like receptor antagonists on methamphetamine and 3,4-methylenedioxymethamphetamine self-administration in rats. Behav Pharmacol 20:688–694

Cagniard B, Sotnikova TD, Gainetdinov RR, Zhuang X (2014) The dopamine transporter expression level differentially affects responses to cocaine and amphetamine. J Neurogenet 28:112–121

Caine SB, Thomsen M, Gabriel KI, Berkowitz JS, Gold LH, Koob GF, Tonegawa S, Zhang J, Xu M (2007) Lack of self-administration of cocaine in dopamine D1 receptor knock-out mice. J Neurosci 27:13140–13150

Carati C, Schenk S (2011) Role of dopamine D1- and D2-like receptor mechanisms in drug-seeking following methamphetamine self-administration in rats. Pharmacol Biochem Behav 98:449–454

Chakrabarti S, Chang A, Liu NJ, Gintzler AR (2016) Chronic opioid treatment augments caveolin-1 scaffolding: relevance to stimulatory mu-opioid receptor adenylyl cyclase signaling. J Neurochem 139:737–747

Chaudhri N, Sahuque LL, Janak PH (2009) Ethanol seeking triggered by environmental context is attenuated by blocking dopamine D1 receptors in the nucleus accumbens core and shell in rats. Psychopharmacology 207:303–314

Chen J, Rusnak M, Lombroso PJ, Sidhu A (2009) Dopamine promotes striatal neuronal apoptotic death via ERK signaling cascades. Eur J Neurosci 29:287–306

Cohen AW, Park DS, Woodman SE, Williams TM, Chandra M, Shirani J, Pereira de Souza A, Kitsis RN, Russell RG, Weiss LM, Tang B, Jelicks LA, Factor SM, Shtutin V, Tanowitz HB, Lisanti MP (2003) Caveolin-1 null mice develop cardiac hypertrophy with hyperactivation of p42/44 MAP kinase in cardiac fibroblasts. Am J Physiol Cell Physiol 284:C457–474

Cremona ML, Matthies HJ, Pau K, Bowton E, Speed N, Lute BJ, Anderson M, Sen N, Robertson SD, Vaughan RA, Rothman JE, Galli A, Javitch JA, Yamamoto A (2011) Flotillin-1 is essential for PKC-triggered endocytosis and membrane microdomain localization of DAT. Nat Neurosci 14:469–477

Cui W, Ren Y, Wang S, Zeng M, Han S, Li J, Han R (2018) The role of caveolin-1 in morphine-induced structural plasticity in primary cultured mouse cerebral cortical neurons. Neurosci Lett 665:38–42

Dumartin B, Jaber M, Gonon F, Caron MG, Giros B, Bloch B (2000) Dopamine tone regulates D1 receptor trafficking and delivery in striatal neurons in dopamine transporter-deficient mice. Proc Natl Acad Sci USA 97:1879–1884

Engelman JA, Chu C, Lin A, Jo H, Ikezu T, Okamoto T, Kohtz DS, Lisanti MP (1998) Caveolin-mediated regulation of signaling along the p42/44 MAP kinase cascade in vivo. A role for the caveolin-scaffolding domain. FEBS Lett 428:205–211

Engelman JA, Zhang XL, Razani B, Pestell RG, Lisanti MP (1999) p42/44 MAP kinase-dependent and -independent signaling pathways regulate caveolin-1 gene expression. Activation of Ras-MAP kinase and protein kinase a signaling cascades transcriptionally down-regulates caveolin-1 promoter activity. J Biol Chem 274:32333–32341

Evans WET, Coyer RL, Sandusky MF, Van Fleet MJ, Moore JG, Nyquist SE (2003) Characterization of membrane rafts isolated from rat sertoli cell cultures: caveolin and flotillin-1 content. J Androl 24:812–821

Fasano C, Bourque MJ, Lapointe G, Leo D, Thibault D, Haber M, Kortleven C, Desgroseillers L, Murai KK, Trudeau LE (2013) Dopamine facilitates dendritic spine formation by cultured striatal medium spiny neurons through both D1 and D2 dopamine receptors. Neuropharmacology 67:432–443

Fenu S, Spina L, Rivas E, Longoni R, Di Chiara G (2006) Morphine-conditioned single-trial place preference: role of nucleus accumbens shell dopamine receptors in acquisition, but not expression. Psychopharmacology 187:143–153

Galbiati F, Volonte D, Engelman JA, Watanabe G, Burk R, Pestell RG, Lisanti MP (1998) Targeted downregulation of caveolin-1 is sufficient to drive cell transformation and hyperactivate the p42/44 MAP kinase cascade. Embo J 17:6633–6648

Galinato MH, Orio L, Mandyam CD (2015) Methamphetamine differentially affects BDNF and cell death factors in anatomically defined regions of the hippocampus. Neuroscience 286:97–108

Galinato MH, Lockner JW, Fannon-Pavlich MJ, Sobieraj JC, Staples MC, Somkuwar SS, Ghofranian A, Chaing S, Navarro AI, Joea A, Luikart BW, Janda KD, Heyser C, Koob GF, Mandyam

CD (2018a) A synthetic small-molecule Isoxazole-9 protects against methamphetamine relapse. Mol Psychiatry 23:629–638
Galinato MH, Takashima Y, Fannon MJ, Quach LW, Morales Silva RJ, Mysore KK, Terranova MJ, Dutta RR, Ostrom RW, Somkuwar SS, Mandyam CD (2018b) Neurogenesis during abstinence is necessary for context-driven methamphetamine-related memory. J Neurosci 38:2029–2042
Gao X, Wu D, Dou L, Zhang H, Huang L, Zeng J, Zhang Y, Yang C, Li H, Liu L, Ma B, Yuan Q (2019) Protective effects of mesenchymal stem cells overexpressing extracellular regulating kinase 1/2 against stroke in rats. Brain Res Bull 149:42–52
Gerfen CR, Young WS 3rd (1988) Distribution of striatonigral and striatopallidal peptidergic neurons in both patch and matrix compartments: an in situ hybridization histochemistry and fluorescent retrograde tracing study. Brain Res 460:161–167
Ghisi V, Ramsey AJ, Masri B, Gainetdinov RR, Caron MG, Salahpour A (2009) Reduced D2-mediated signaling activity and transsynaptic upregulation of D1 and D2 dopamine receptors in mice overexpressing the dopamine transporter. Cell Signal 21:87–94
Giros B, Jaber M, Jones SR, Wightman RM, Caron MG (1996) Hyperlocomotion and indifference to cocaine and amphetamine in mice lacking the dopamine transporter. Nature 379:606–612
Gong X, Yue K, Ma B, Xing J, Gan Y, Wang D, Jin G, Li C (2016) Levo-tetrahydropalmatine, a natural, mixed dopamine receptor antagonist, inhibits methamphetamine self-administration and methamphetamine-induced reinstatement. Pharmacol Biochem Behav 144:67–72
Gross NB, Duncker PC, Marshall JF (2011) Striatal dopamine D1 and D2 receptors: widespread influences on methamphetamine-induced dopamine and serotonin neurotoxicity. Synapse 65:1144–1155
Haberny SL, Berman Y, Meller E, Carr KD (2004) Chronic food restriction increases D-1 dopamine receptor agonist-induced phosphorylation of extracellular signal-regulated kinase 1/2 and cyclic AMP response element-binding protein in caudate-putamen and nucleus accumbens. Neuroscience 125:289–298
He Y, Yu LP, Jin GZ (2009) Differential distributions and trafficking properties of dopamine D1 and D5 receptors in nerve cells. Neurosci Bull 25:43–53
Head BP, Hu Y, Finley JC, Saldana MD, Bonds JA, Miyanohara A, Niesman IR, Ali SS, Murray F, Insel PA, Roth DM, Patel HH, Patel PM (2011) Neuron-targeted caveolin-1 protein enhances signaling and promotes arborization of primary neurons. J Biol Chem 286:33310–33321
Ince E, Ciliax BJ, Levey AI (1997) Differential expression of D1 and D2 dopamine and m4 muscarinic acetylcholine receptor proteins in identified striatonigral neurons. Synapse 27:357–366
Jaramillo AA, Randall PA, Stewart S, Fortino B, Van Voorhies K, Besheer J (2018) Functional role for cortical-striatal circuitry in modulating alcohol self-administration. Neuropharmacology 130:42–53
Jiao H, Zhang L, Gao F, Lou D, Zhang J, Xu M (2007) Dopamine D(1) and D(3) receptors oppositely regulate NMDA- and cocaine-induced MAPK signaling via NMDA receptor phosphorylation. J Neurochem 103:840–848
Johnson PM, Kenny PJ (2010) Dopamine D2 receptors in addiction-like reward dysfunction and compulsive eating in obese rats. Nat Neurosci 13:635–641
Jones SR, Gainetdinov RR, Jaber M, Giros B, Wightman RM, Caron MG (1998) Profound neuronal plasticity in response to inactivation of the dopamine transporter. Proc Natl Acad Sci USA 95:4029–4034
Kang MJ, Chung YH, Hwang CI, Murata M, Fujimoto T, Mook-Jung IH, Cha CI, Park WY (2006) Caveolin-1 upregulation in senescent neurons alters amyloid precursor protein processing. Exp Mol Med 38:126–133
Kim A, Mandyam CD (2014) Methamphetamine affects cell proliferation in the medial prefrontal cortex: a new niche for toxicity. Pharmacol Biochem Behav 126:90–96
Kong MM, Hasbi A, Mattocks M, Fan T, O'Dowd BF, George SR (2007) Regulation of D1 dopamine receptor trafficking and signaling by caveolin-1. Mol Pharmacol 72:1157–1170
Kreisler AD, Garcia MG, Spierling SR, Hui BE, Zorrilla EP (2017) Extended vs. brief intermittent access to palatable food differently promote binge-like intake, rejection of less preferred food, and weight cycling in female rats. Physiol Behav 177:305–316
Kreisler AD, Mattock M, Zorrilla EP (2018) The duration of intermittent access to preferred sucrose-rich food affects binge-like intake, fat accumulation, and fasting glucose in male rats. Appetite 130:59–69
Kruyer A, Scofield MD, Wood D, Reissner KJ, Kalivas PW (2019) Heroin cue-evoked astrocytic structural plasticity at nucleus accumbens synapses inhibits heroin seeking. Biol Psychiatry 86:811–819
Lindgren N, Goiny M, Herrera-Marschitz M, Haycock JW, Hokfelt T, Fisone G (2002) Activation of extracellular signal-regulated kinases 1 and 2 by depolarization stimulates tyrosine hydroxylase phosphorylation and dopamine synthesis in rat brain. Eur J Neurosci 15:769–773
Liu Y, Young KA, Curtis JT, Aragona BJ, Wang Z (2011) Social bonding decreases the rewarding properties of amphetamine through a dopamine D1 receptor-mediated mechanism. J Neurosci 31:7960–7966
Lobo MK, Nestler EJ (2011) The striatal balancing act in drug addiction: distinct roles of direct and indirect pathway medium spiny neurons. Front Neuroanat 5:41
Lobo MK, Covington HE 3rd, Chaudhury D, Friedman AK, Sun H, Damez-Werno D, Dietz DM, Zaman S, Koo JW, Kennedy PJ, Mouzon E, Mogri M, Neve RL, Deisseroth K, Han MH, Nestler EJ (2010) Cell type-specific loss of BDNF signaling mimics optogenetic control of cocaine reward. Science 330:385–390
Lynch WJ (2006) Sex differences in vulnerability to drug self-administration. Exp Clin Psychopharmacol 14:34–41
Mandyam CD, Norris RD, Eisch AJ (2004) Chronic morphine induces premature mitosis of proliferating cells in the adult mouse subgranular zone. J Neurosci Res 76:783–794
Mandyam CD, Wee S, Eisch AJ, Richardson HN, Koob GF (2007) Methamphetamine self-administration and voluntary exercise have opposing effects on medial prefrontal cortex gliogenesis. J Neurosci 27:11442–11450
Mandyam CD, Schilling JM, Cui W, Egawa J, Niesman IR, Kellerhals SE, Staples MC, Busija AR, Risbrough VB, Posadas E, Grogman GC, Chang JW, Roth DM, Patel PM, Patel HH, Head BP (2015) Neuron-targeted caveolin-1 improves molecular signaling, plasticity, and behavior dependent on the hippocampus in adult and aged mice. Biol Psychiatry 81:101–110
Mastrangelo L, Kim JE, Miyanohara A, Kang TH, Friedmann T (2012) Purinergic signaling in human pluripotent stem cells is regulated by the housekeeping gene encoding hypoxanthine guanine phosphoribosyltransferase. Proc Natl Acad Sci USA 109:3377–3382
Mizoguchi H, Yamada K, Mizuno M, Mizuno T, Nitta A, Noda Y, Nabeshima T (2004) Regulations of methamphetamine reward by extracellular signal-regulated kinase 1/2/ets-like gene-1 signaling pathway via the activation of dopamine receptors. Mol Pharmacol 65:1293–1301
Morgan D, Brebner K, Lynch WJ, Roberts DC (2002) Increases in the reinforcing efficacy of cocaine after particular histories of reinforcement. Behav Pharmacol 13:389–396
Nestler EJ (2001) Molecular basis of long-term plasticity underlying addiction. Nat Rev Neurosci 2:119–128
Nguyen JD, Aarde SM, Cole M, Vandewater SA, Grant Y, Taffe MA (2016) Locomotor stimulant and rewarding effects of inhaling

methamphetamine, MDPV, and mephedrone via electronic cigarette-type technology. Neuropsychopharmacology 41:2759–2771
Noonan MA, Bulin SE, Fuller DC, Eisch AJ (2010) Reduction of adult hippocampal neurogenesis confers vulnerability in an animal model of cocaine addiction. J Neurosci 30:304–315
Noori-Daloii MR, Mojarrad M, Rashidi-Nezhad A, Kheirollahi M, Shahbazi A, Khaksari M, Korzebor A, Goodarzi A, Ebrahimi M, Noori-Daloii AR (2012) Use of siRNA in knocking down of dopamine receptors, a possible therapeutic option in neuropsychiatric disorders. Mol Biol Rep 39:2003–2010
Oliver RJ, Purohit DC, Kharidia KM, Mandyam CD (2019) Transient chemogenetic inhibition of D1-MSNs in the dorsal striatum enhances methamphetamine self-administration. Brain Sci 9:e330
Piazza PV, Deminiere JM, Le Moal M, Simon H (1989) Factors that predict individual vulnerability to amphetamine self-administration. Science 245:1511–1513
Piazza PV, Deroche-Gamonent V, Rouge-Pont F, Le Moal M (2000) Vertical shifts in self-administration dose–response functions predict a drug-vulnerable phenotype predisposed to addiction. J Neurosci 20:4226–4232
Porras G, Berthet A, Dehay B, Li Q, Ladepeche L, Normand E, Dovero S, Martinez A, Doudnikoff E, Martin-Negrier ML, Chuan Q, Bloch B, Choquet D, Boue-Grabot E, Groc L, Bezard E (2012) PSD-95 expression controls L-DOPA dyskinesia through dopamine D1 receptor trafficking. J Clin Invest 122:3977–3989
Rajendran L, Le Lay S, Illges H (2007) Raft association and lipid droplet targeting of flotillins are independent of caveolin. Biol Chem 388:307–314
Richardson NR, Roberts DC (1996) Progressive ratio schedules in drug self-administration studies in rats: a method to evaluate reinforcing efficacy. J Neurosci Methods 66:1–11
Roberts DC (1993) Self-administration of GBR 12909 on a fixed ratio and progressive ratio schedule in rats. Psychopharmacology 111:202–206
Roberts DC, Loh EA, Vickers G (1989) Self-administration of cocaine on a progressive ratio schedule in rats: dose–response relationship and effect of haloperidol pretreatment. Psychopharmacology 97:535–538
Robison LS, Ananth M, Hadjiargyrou M, Komatsu DE, Thanos PK (2017) Chronic oral methylphenidate treatment reversibly increases striatal dopamine transporter and dopamine type 1 receptor binding in rats. J Neural Trans (Vienna, Austria: 1996) 124:655–667
Rospond B, Sadakierska-Chudy A, Kazek G, Krosniak M, Bystrowska B, Filip M (2019) Assessment of metabolic and hormonal profiles and striatal dopamine D2 receptor expression following continuous or scheduled high-fat or high-sucrose diet in rats. Pharmacol Rep 71:1–12
Rui G, Guangjian Z, Yong W, Jie F, Yanchao C, Xi J, Fen L (2013) High frequency electro-acupuncture enhances striatum DAT and D1 receptor expression, but decreases D2 receptor level in 6-OHDA lesioned rats. Behav Brain Res 237:263–269
Rupniak NM, Briggs RS, Petersen MM, Mann S, Reavill C, Jenner P, Marsden CD (1986) Differential alterations in striatal acetylcholine function in rats during 12 months' continuous administration of haloperidol, sulpiride, or clozapine. Clin Neuropharmacol 9:282–292
Salahpour A, Ramsey AJ, Medvedev IO, Kile B, Sotnikova TD, Holmstrand E, Ghisi V, Nicholls PJ, Wong L, Murphy K, Sesack SR, Wightman RM, Gainetdinov RR, Caron MG (2008) Increased amphetamine-induced hyperactivity and reward in mice overexpressing the dopamine transporter. Proc Natl Acad Sci USA 105:4405–4410
Sase A, Aher YD, Saroja SR, Ganesan MK, Sase S, Holy M, Hoger H, Bakulev V, Ecker GF, Langer T, Sitte HH, Leban J, Lubec G (2016) A heterocyclic compound CE-103 inhibits dopamine reuptake and modulates dopamine transporter and dopamine D1–D3 containing receptor complexes. Neuropharmacology 102:186–196
Schwendt M, Rocha A, See RE, Pacchioni AM, McGinty JF, Kalivas PW (2009) Extended methamphetamine self-administration in rats results in a selective reduction of dopamine transporter levels in the prefrontal cortex and dorsal striatum not accompanied by marked monoaminergic depletion. J Pharmacol Exp Ther 331:555–562
Segal DS, Kuczenski R, O'Neil ML, Melega WP, Cho AK (2005) Prolonged exposure of rats to intravenous methamphetamine: behavioral and neurochemical characterization. Psychopharmacology 180:501–512
Shen J, Li Y, Qu C, Xu L, Sun H, Zhang J (2019) The enriched environment ameliorates chronic unpredictable mild stress-induced depressive-like behaviors and cognitive impairment by activating the SIRT1/miR-134 signaling pathway in hippocampus. J Affect Disord 248:81–90
Shi X, McGinty JF (2011) D1 and D2 dopamine receptors differentially mediate the activation of phosphoproteins in the striatum of amphetamine-sensitized rats. Psychopharmacology 214:653–663
Shippenberg TS, Bals-Kubik R, Herz A (1993) Examination of the neurochemical substrates mediating the motivational effects of opioids: role of the mesolimbic dopamine system and D-1 vs. D-2 dopamine receptors. J Pharmacol Exp Ther 265:53–59
Somkuwar SS, Fannon MJ, Head BP, Mandyam CD (2016) Methamphetamine reduces expression of caveolin-1 in the dorsal striatum: implication for dysregulation of neuronal function. Neuroscience 328:147–156
Song Z, Kalyani M, Becker JB (2018) Sex differences in motivated behaviors in animal models. Curr Opin Behav Sci 23:98–102
Spielewoy C, Biala G, Roubert C, Hamon M, Betancur C, Giros B (2001) Hypolocomotor effects of acute and daily d-amphetamine in mice lacking the dopamine transporter. Psychopharmacology 159:2–9
Spina L, Fenu S, Longoni R, Rivas E, Di Chiara G (2006) Nicotine-conditioned single-trial place preference: selective role of nucleus accumbens shell dopamine D1 receptors in acquisition. Psychopharmacology 184:447–455
Stary CM, Tsutsumi YM, Patel PM, Head BP, Patel HH, Roth DM (2012) Caveolins: targeting pro-survival signaling in the heart and brain. Front Physiol 3:393
Sun W, Ginovart N, Ko F, Seeman P, Kapur S (2003) In vivo evidence for dopamine-mediated internalization of D2-receptors after amphetamine: differential findings with [3H]raclopride versus [3H]spiperone. Mol Pharmacol 63:456–462
Sun J, Xu J, Cairns NJ, Perlmutter JS, Mach RH (2012) Dopamine D1, D2, D3 receptors, vesicular monoamine transporter type-2 (VMAT2) and dopamine transporter (DAT) densities in aged human brain. PLoS ONE 7:e49483
Tonissaar M, Herm L, Rinken A, Harro J (2006) Individual differences in sucrose intake and preference in the rat: circadian variation and association with dopamine D2 receptor function in striatum and nucleus accumbens. Neurosci Lett 403:119–124
Turner C, De Luca M, Wolfheimer J, Hernandez N, Madsen KL, Schmidt HD (2020) Administration of a novel high affinity PICK1 PDZ domain inhibitor attenuates cocaine seeking in rats. Neuropharmacology 164:107901
Vazquez D, Pribut HJ, Burton AC, Tennyson SS, Roesch MR (2019) Prior cocaine self-administration impairs attention signals in anterior cingulate cortex. Neuropsychopharmacology 45:833–841
Voulalas PJ, Schetz J, Undieh AS (2011) Differential subcellular distribution of rat brain dopamine receptors and subtype-specific redistribution induced by cocaine. Mol Cell Neurosci 46:645–654

Wise RA (2006) Role of brain dopamine in food reward and reinforcement. Philos Trans R Soc Lond B Biol Sci 361:1149–1158

Worsley JN, Moszczynska A, Falardeau P, Kalasinsky KS, Schmunk G, Guttman M, Furukawa Y, Ang L, Adams V, Reiber G, Anthony RA, Wickham D, Kish SJ (2000) Dopamine D1 receptor protein is elevated in nucleus accumbens of human, chronic methamphetamine users. Mol Psychiatry 5:664–672

Xi ZX, Kleitz HK, Deng X, Ladenheim B, Peng XQ, Li X, Gardner EL, Stein EA, Cadet JL (2009) A single high dose of methamphetamine increases cocaine self-administration by depletion of striatal dopamine in rats. Neuroscience 161:392–402

Yao WD, Gainetdinov RR, Arbuckle MI, Sotnikova TD, Cyr M, Beaulieu JM, Torres GE, Grant SG, Caron MG (2004) Identification of PSD-95 as a regulator of dopamine-mediated synaptic and behavioral plasticity. Neuron 41:625–638

Yin WL, Yin WG, Huang BS, Wu LX (2017) Neuroprotective effects of lentivirus-mediated cystathionine-beta-synthase overexpression against 6-OHDA-induced Parkinson's disease rats. Neurosci Lett 657:45–52

Young EA, Dreumont SE, Cunningham CL (2014) Role of nucleus accumbens dopamine receptor subtypes in the learning and expression of alcohol-seeking behavior. Neurobiol Learn Mem 108:28–37

Yu P, Villar VA, Jose PA (2013) Methods for the study of dopamine receptors within lipid rafts of kidney cells. Methods Mol Biol 964:15–24

Zhang J, Saur T, Duke AN, Grant SG, Platt DM, Rowlett JK, Isacson O, Yao WD (2014) Motor impairments, striatal degeneration, and altered dopamine-glutamate interplay in mice lacking PSD-95. J Neurogenet 28:98–111